Electronic Supplementary Information for

Silver (I) metal-organic framework-embedded polylactic acid electrospun fibrous membranes for efficient inhibition of bacteria

Siqi Zhang [a], Xiao Ma [a], Hailong Yu [a], Xinyi Lu [a, b], Jianhui Liu [b], Lihua Zhang [b], Guangyao Wang [a], Junwei Ye *, [a], Guiling Ning *, [a]

[a] State Key Laboratory of Fine Chemicals, School of Chemical Engineering, Dalian University of Technology, 2 Linggong Road, Dalian, Liaoning, 116024, PR China

[b] CAS Key Laboratory of Separation Sciences for Analytical Chemistry, Dalian Institute of Chemical Physics, Chinese Academy of Sciences, Dalian 116023, PR China

***Corresponding author**

Email Address: junweiye@dlut.edu.cn (J. W. Ye), ninggl@dlut.edu.cn (G. L. Ning).

1. Experiment section

1.1. Proteomics analysis

Proteomic analysis was carried out according to a previous reported literature. [1]

1.1.1 Proteome sample preparation

The proteins were extracted by the lysis buffer containing 1% (v/v) protease inhibitor cocktail in 8 M urea. The extracted proteins were then sonicated using Bioruptor Pico Ultrasonicator (Diagenode). Dithiothreitol (DTT) were added to reduce disulfide bonds and the proteins were incubated at 56°C for 1 h. Iodoacetamide (IAA) were added for protein alkylation and incubated for 30 min in darkness. Phosphate buffer (PB, pH 8.0, 50 mM) were further added to dilute the solution to 1 M urea. Proteins were digested by trypsin with the ratio of 1:50 enzyme/protein at 37 °C overnight.

1.1.2 LC−MS/MS analysis

Peptides were separated on a 15 cm reversed phase column (packed in-house with ReproSil-Pur C18-AQ 1.9 μm [Dr. Maisch GmbH]) on an ultra-HPLC EASY-nLC 1000 system (Thermo Fisher Scientific). Separation gradient was 5−22% B (0.1−110.1 min), 22−35% B (110.1−135.1 min), 35−80% B (135.1−135.2 min) with buffer A (98% H_2O, 2% ACN, 0.1% FA) and buffer B (2% H_2O, 98% ACN, 0.1% FA).The data were acquired on a Q Exactive mass spectrometer (Thermo Fisher Scientific) in a data-dependent mode. Full scan was acquired in the Orbitrap at a resolution of 70 000 from 300 to 1800 m/z and an AGC target was 1×10^6 within a maximum injection time of 50 ms. Ions were sequentially isolated by quadrupole using a 2.0 m/z isolation window to a target value of 1×10^5 and a maximum injection time 100 ms. Then they were fragmented by HCD (normalized collision energy of 28%) and detected by Orbitrap at 17 500 resolution. Loop count was 20. The exclusion duration was 45s.

1.1.3 Data processing

All raw files were analyzed together by Andromeda for database search in the MaxQuant environment v.1.6.1.0. MS/MS spectra were searched against the *E. coli* protein database (UniProt Proteome, release 2018_07). Enzyme specificity was set to trypsin with up to two missed cleavages. Carbamidomethylation (C) (+57.021 Da) was set as fixed modification. Oxidation (M) (+15.995 Da) and acetylation (protein N-termini) (+42.011 Da) were set as variable modifications. The mass tolerances were 10 ppm for the precursor ions and 20 ppm for the fragment ions. We used 'match between runs' in the time window of 2 min. The quantification results were based on the intensities of label free quantification method.

1.2. Statistical analysis

All the quantitative data in this paper were shown as means ±standard deviations with n=3. The statistical analysis was performed using Origin 2021 software. Comparisons between groups were analyzed by one-way analysis of variance (ANOVA).

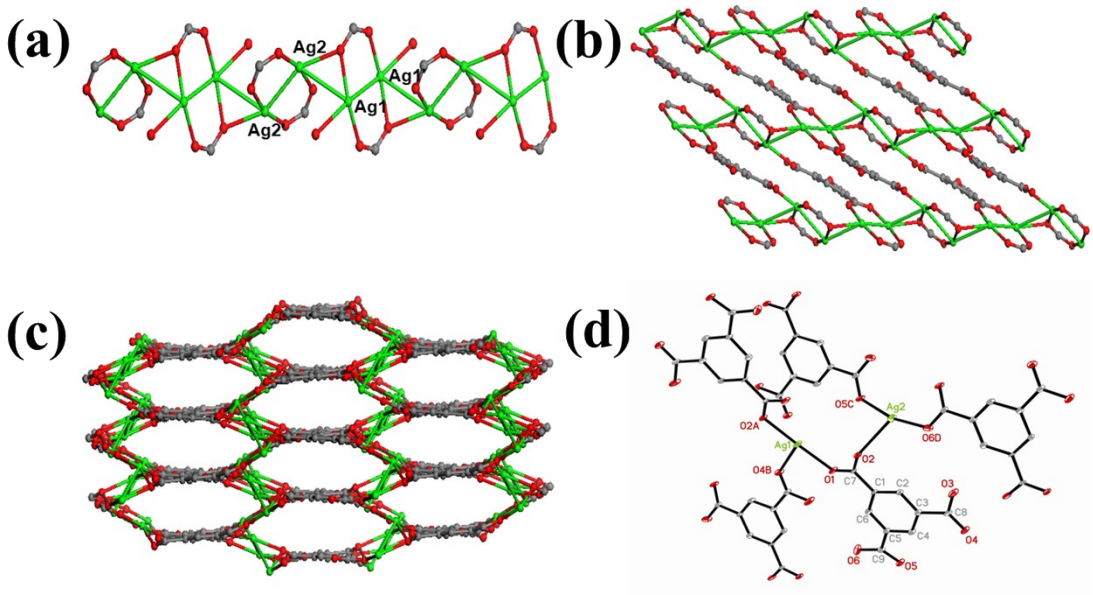

Fig. S1 View of the (a) rod-shaped building blocks, (b) layers, (c) 3-D frameworks of Ag_2(HBTC), (d) perspective view of the coordination environment of the Ag (I) centers in Ag_2(HBTC) with atoms represented by 30% thermal ellipsoids.

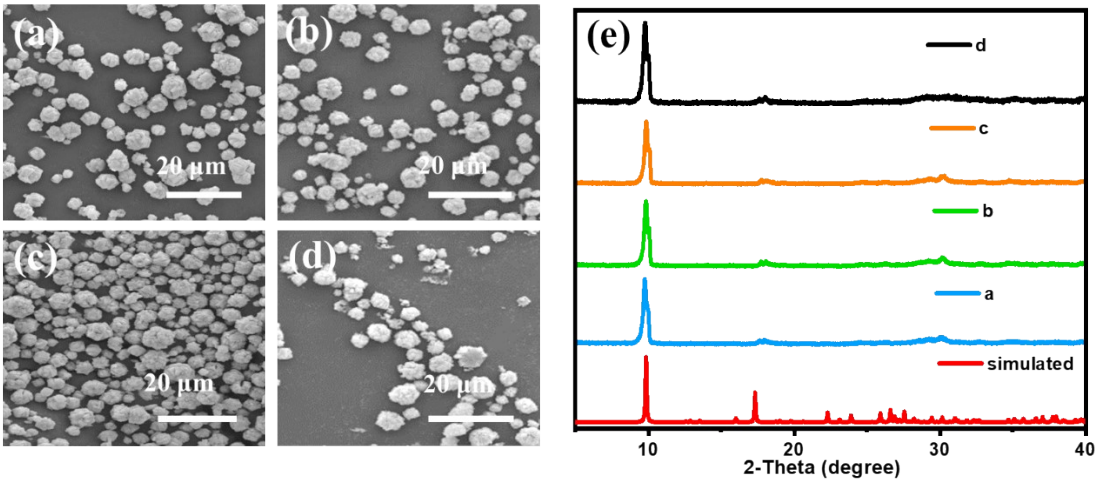

Fig. S2 SEM images of nanoscale Ag_2(HBTC) synthesized through emulsion-templating method at (a) 120 ℃ for 0.5 h, (b) 120 ℃ for 1.0 h, (c) 160 ℃ for 0.5 h and (d) 160 ℃ for 1.0 h. (e) XRD patterns for the simulated and synthesized Ag_2(HBTC) in Figure S2a-d.

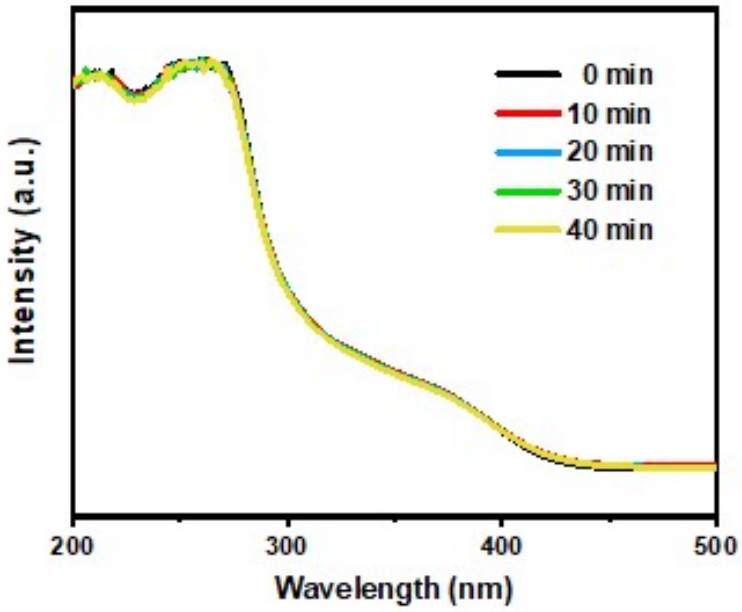

Fig. S3 Time-dependent UV-vis spectra of NBT under Xenon lamp irradiation.

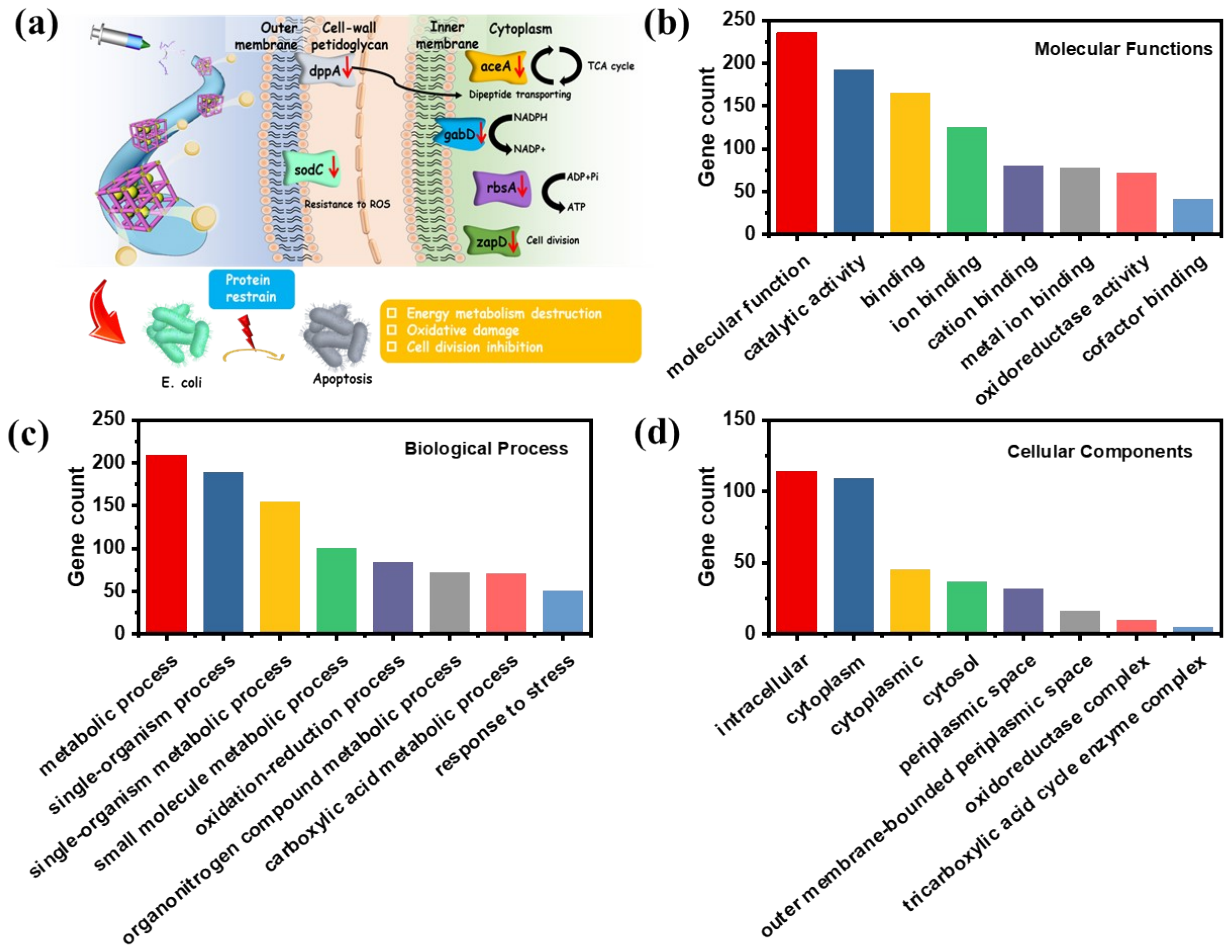

Fig. S4 (a) Schematic of the potential antibacterial mechanism concluded from the proteomic analysis. The differentially expressed proteins classified using Gene Ontology annotation into (b) molecular functions, (c) biological process and (d) cellular components.

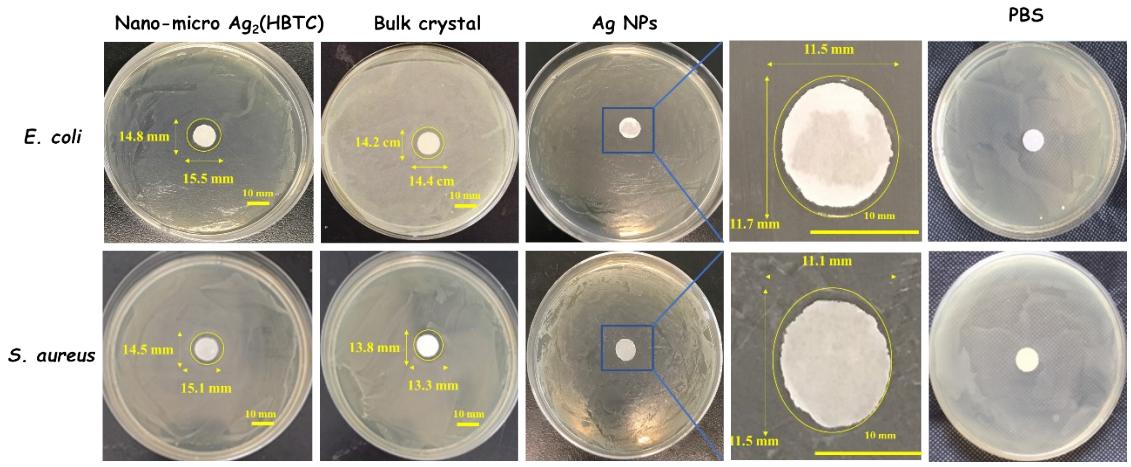

Fig. S5 Optical images of inhibition zone treated with nano-micro scale Ag_2(HBTC), bulk crystal, Ag NPs and PBS against *E. coli* and *S. aureus*.

Table S1. Selected bond lengths [Å] for Ag_2(HBTC)

[Ag_2(HBTC)]			
Ag(1)-O(1)	2.233(4)	Ag(1)-O(2)$^{\#1}$	2.244(4)
Ag(1)-O(4)$^{\#2}$	2.546(4)	Ag(1)-Ag(1)$^{\#1}$	2.8622(10)
Ag(1)-Ag(2)$^{\#1}$	3.2276(8)	Ag(2)-O(6)$^{\#3}$	2.127(5)
Ag(2)-O(5)$^{\#4}$	2.170(4)	Ag(2)-O(2)	2.537(5)
Ag(2)-Ag(2)$^{\#5}$	2.8184(11)	Ag(2)-Ag(1)$^{\#1}$	3.2276(8)

Symmetry transformations used to generate equivalent atoms: #1 -x+1, -y, -z+1, #2 x+1, -y+1/2, z+1/2, #3 x-1, -y+1/2, z-1/2, #4 -x+1, y-1/2, -z+1/2, #5 -x, -y, -z

Table S2. Selected bond angles [°] for Ag_2(HBTC)

[Ag_2(HBTC)]			
O(1)-Ag(1)-O(2)$^{\#1}$	161.41(16)	O(6)$^{\#3}$-Ag(2)-O(5)$^{\#4}$	164.57(19)
O(1)-Ag(1)-O(4)$^{\#2}$	86.15(15)	O(6)$^{\#3}$-Ag(2)-O(2)	113.58(17)
O(2)$^{\#1}$-Ag(1)-O(4)$^{\#2}$	108.28(15)	O(5)$^{\#4}$-Ag(2)-O(2)	81.29(16)
O(1)-Ag(1)-Ag(1)$^{\#1}$	79.63(11)	O(6)$^{\#3}$-Ag(2)-Ag(2)$^{\#5}$	84.70(13)
O(2)$^{\#1}$-Ag(1)-Ag(1)$^{\#1}$	83.38(10)	O(5)$^{\#4}$-Ag(2)-Ag(2)$^{\#5}$	79.90(12)
O(4)$^{\#2}$-Ag(1)-Ag(1)$^{\#1}$	160.16(11)	O(2)-Ag(2)-Ag(2)$^{\#5}$	153.66(10)
O(1)-Ag(1)-Ag(2)$^{\#1}$	131.90(13)	O(6)$^{\#3}$-Ag(2)-Ag(1)$^{\#1}$	131.74(18)
O(2)$^{\#1}$-Ag(1)-Ag(2)$^{\#1}$	51.50(12)	O(5)$^{\#4}$-Ag(2)-Ag(1)$^{\#1}$	56.22(14)
O(4)$^{\#2}$-Ag(1)-Ag(2)$^{\#1}$	63.92(12)	O(2)-Ag(2)-Ag(1)$^{\#1}$	43.80(10)
Ag(1)$^{\#1}$-Ag(1)-Ag(2)$^{\#1}$	116.78(3)	Ag(2)$^{\#5}$-Ag(2)-Ag(1)$^{\#1}$	109.92(3)

Symmetry transformations used to generate equivalent atoms: #1 -x+1, -y, -z+1, #2 x+1, -y+1/2, z+1/2, #3 x-1, -y+1/2, z-1/2, #4 -x+1, y-1/2, -z+1/2, #5 -x, -y, -z

Table S3. Crystallographic Data and Structure Refinements for Ag_2(HBTC)

	Ag_2(HBTC)
Empirical formula	$C_9H_4O_6Ag_2$
Formula weight	423.86
Crystal system	Monoclinic
Space group	*P21/c*
a (Å)	7.0523(4)
b (Å)	17.9550(11)
c (Å)	7.4629(5)
β (º)	94.820(2)
Volume (Å^3)	941.64(10)
Z	4
*D*calc（mg/m^{-3}）	2.990
μ (mm^{-1})	4.172
$F_{(000)}$	800
R_{int}	0.1930
GOF on F^2	1.161
R_1 [I>2σ (*I*)]*	0.0551
wR_2 [I>2σ (*I*)]*	0.1352
R_1 (all data) *	0.0569
wR_2 (all data)*	0.1366

*$R_1 = \Sigma||F_o|-|F_c||/\Sigma|F_o|$; $wR_2 = \{\Sigma[w(F_o^2-F_c^2)^2]/\Sigma[w(F_o^2)]^2\}^{1/2}$

Table S4. Antibacterial properties of MOFs based composites.

Materials	Synthesis approach	Bacteria strains	Antibacterial efficiency	Experimental methods	Mechanism Investigation	Reference
Ag-MOF/polyamide	In-situ growth	*E. coli*	76.3%	Heterotrophic plate count experiments; Confocal microscopy test; SEM observation	Ag^{+} releasing	2
Cu-MOF/cotton	Post synthetic modification	*E. coli*	⩾4-log reduction (24 h)	Cellular viability	Cu^{2+} releasing	3
ZIF-8@hydrogel	Microfluidic-emulsion-templating method	*E. coli*	99.3% (ZIF-8>500 μg/mL)	Colony counting method	Zinc ion release test	4
Ag-MOFs@CNF@CF	In situ green deposition method	*E. coli*	Inhibition zone 18.1 mm	Inhibition zone test	---	5
MOF-Embedded Hydrogels	UV light-mediated thiol−ene photopolymerization	*E. coli* *S. aurues*	MBC hydrogel@ Cu-MOF 1 and hydrogel@Co-MOF 2: 99.9% hydrogel@Zn-MOF 3 :0%	Colony counting method	Metal ion release test	6
Cu-MOF-1/PLA	Electrospinning	*E. coli* *S. aureus*	*E. coli*: 99.4% *S. aureus*: 99.6%	Growth curve; Colony counting method; Fluorescence-based staining assay; Morphological investigation	Release of Cu^{2+} ions,	7
Cu-MOF-74/PVDF	Coating	*E. coli*	97.7% (Cu-MOF-74 loading amount: 0.05 g)	Colony counting method	Cu^{2+} assays; ROS detection	8
Dimethyl fumarate-loaded-HKUST-1@CMCS	chemically connecting	*E. coli, S.aureus*	Inhibition zone *E. coli*: 12.8 ± 1.4 mm *S. aureus*:17.4 ± 0.1	zone inhibition test	Dimethyl fumarate releasing test; Measurement of Cu(II) level	9
LV@UiO-66-NH_2@PVA	metal complexation and heat treatment.	*E. coli, S.aureus*	higher than 3 log CFU reduction of *E. coli* and *S. aureus* at 100 μg/mL.	Colony counting method Fluorescent-based bacteria live/dead test	---	10
Ag_2(HBTC)/PLA	Emulation templating method; one step electrospinning	*E. coli, S.aureus*	MIC: *E. coli* 50–100 mg/L *S. aureus*: 100–150 mg/L Antibacterial rate: more than 99.9% toward both strains (250 mg/L)	Growth curve, zone of inhibition, Bacterial reduction assay, Morphology investigation Fluorescent-based bacteria live/dead test	Ag^{+} releasing; superoxide species detection; proteomic analysis	This work

References

1. S. Zhang, J. Ye, Y. Sun, J. Kang, J. Liu, Y. Wang, Y. Li, L. Zhang and G. Ning, Chem. Eng. J., 2020, **390**, 124523.

2. M. Pejman, M. D. Firouzjaei, S. A. Aktij, P. Das, E. Zolghadr, H. Jafarian, A. A. Shamsabadi, M. Elliott, M. Sadrzadeh, M. Sangermano, A. Rahimpour and A. Tiraferri, ACS Appl. Mater. Interfaces, 2020, **12**, 36287-36300.

3. H. N. Rubin, B. H. Neufeld and M. M. Reynolds, ACS Appl. Mater. Interfaces, 2018, **10**, 15189-15199.

4. X. Yao, G. Zhu, P. Zhu, J. Ma, W. Chen, Z. Liu and T. Kong, Adv. Funct. Mater., 2020, **30**, 1909389.

5. S. Ma, M. Zhang, J. Nie, J. Tan, B. Yang and S. Song, Carbohydr. Polym., 2019, **203**, 415-422.

6. K. Gwon, I. Han, S. Lee, Y. Kim and D. N. Lee, ACS Appl. Mater. Interfaces, 2020, **12**, 20234-20242.

7. Z. Liu, J. W. Ye, A. Rauf, S. Q. Zhang, G. Y. Wang, S. Q. Shi and G. L. Ning, Biomater. Sci., 2021, **9**, 3851-3859.

8. H. Zheng, D. Wang, X. Sun, S. Jiang, Y. Liu, D. Zhang and L. Zhang, Chem. Eng. J., 2021, **411**, 128524.

9. G. Huang, Y. Li, Z. Qin, Q. Liang, C. Xu and B. Lin, Carbohydr. Polym., 2020, **233**, 115848.

10. J. Zhu, W. Qiu, C. Yao, C. Wang, D. Wu, S. Pradeep, J. Yu and Z. Dai, J. Colloid Interface Sci., 2021, **603**, 243-251.